IJSRM
INTERNATIONAL JOURNAL OF SCIENCE AND RESEARCH METHODOLOGY
An Official Publication of Human Journals

Human Journals
Research Article
May 2021 Vol.:18, Issue:3

Adsorption of Chromium (VI) onto Activated Carbons Prepared from *Raphia farinifera* Fruit Kernels by Chemical Activation with Phosphoric Acid (H_3PO_4)

IJSRM
INTERNATIONAL JOURNAL OF SCIENCE AND RESEARCH METHODOLOGY
An Official Publication of Human Journals

Jacques Bomiko Mbouombouo, Caroline Lincold Nintedem Magapgie, Pierre Gerard Tchieta*, Harlette Zapenaha Poumve, Esther Judith Maffeu, Carine Tsokeng Lannang, Robert Djientieu Leumaleu, Alain Francois Kamdem Waffo

Chemistry Laboratory, Faculty of Science, University of Douala; BP 24157 Douala, Cameroon

Submitted: 21 April 2021
Accepted: 27 April 2021
Published: 30 May 2021

Keywords: Activated carbon, Adsorption, Kinetics, Thermodynamics, Isotherm

ABSTRACT

The objective of this work is to prepare activated carbon from *Raphia farinifera* fruit kernels, having a better porosity and important chemical property for the reduction of chromium (VI) in aqueous medium. The materials were characterized by: thermogravimetric analysis, differential thermal and differential scanning calorimetry (TG-DTG-DSC), Fourier transform infrared (FT-IR), Boehm titration, pH at zero charge point (pH_{PCN}), iodine number (I_{I2}) and methylene blue number (I_{MB}). The evaluation of adsorption capacity involves discussing the effects of contact time, solution pH and the effect of temperature using a batch adsorption technique. In addition, different kinetic models (first and second order and intra-particle) and adsorption isotherms (Langmuir, Freundlich) were applied. Analysis of the TGA curve illustrates the presence of hemicellulose, cellulose and lignin thus confirming the lignocellulosic structure. The surface of three activated carbons could be mainly acidic but also weakly basic with regard to pH_{PCN}, analysis of surface chemical function by Boehm and FT-IR titration (-OH, $-NH_2$, C=O, –COO- and –COOH). These exhibit microporosity and mesoporosity on their surfaces. The value: of pH_{PCN} (5.63, 5.83 and 5.66) present an acidic surface, of the iodine number I_2 (913.716, 939.097 and 964.478 mg. g^{-1}) indicates a better microposity, of the I_{MB} methylene blue number (322.58, 344.83 and 476.19 mg. g^{-1}) justifies a better mesoporosity and specific surface area of methylene blue (S_{MB} = 1063.74, 1136.12 and 1568, 92 m^2. g^{-1}) shows a very large exchange surface of AC1/1, AC1/2 and AC1/3, respectively. The pseudo-second order kinetic model better describes the adsorption of chromium (VI) on AC, with R^2 = 1 for AC1/1 and AC1/2 and R^2 = 0.999 for AC1/3. The Langmuir and Freundlich model better describes the adsorption of chromium (VI) on AC, with $R_L \leq 0.342$ and $K_f \geq 5.150$. The thermodynamic study gave the negative values of the free energy which justify the feasibility and the spontaneous nature of the process of adsorption of chromium (VI) on AC, the negative values of the free enthalpy and the entropy translate that the adsorption process is exothermic and indicates an increase in order at the solid/liquid interface. The low values of the free enthalpy ($\Delta H° < 0$ kJ mol^{-1}) indicate that the chromium (VI) adsorption process on all ACs is physical.

INTRODUCTION

The protection of the environment has become a major issue, at the same time as the idea of its degradation, both global and local, has emerged, due to industrial and human activities. At the present times, the contamination is even affecting the freshwater which is found deteriorated by various pollutants from various sources: industries, intensive agriculture, transport, domestic waste, health products, urban waste, water soluble air pollution [1].

The main sources of chromium (VI) in the environment are of anthropogenic origins such as non-ferrous metal smelters, refineries, tanneries, urban stormwater discharges, pulp mill effluents and paper and waste from thermal power stations [2]. Chromium (VI) enters the human body primarily through drinking water, followed by food, dust, air and soil. Chromium (VI) causes cancer of the stomach or lungs, abnormal sperm morphologies in men, gastrointestinal, respiratory, liver and kidney damage. According to the Federal-Provincial-Territorial Committee on Drinking Water (CEP), the maximum acceptable concentration (MAC) of chromium (VI) in drinking water is 0.1 mg / L (100 µg / L) [3].

Adsorption remains one of the most widely used pollutant removal techniques due to its efficiency, ease of implementation and affordable investment cost. This method requires the choice of an adsorbent with good chemical and textural properties such as zeolites or polymer resins, silica gels, activated aluminas, activated carbon (AC) [4].

Activated carbons are preferentially mentioned among the many adsorbent materials generally used in aqueous or gaseous medium for the adsorption of organic compounds (depollution, discoloration and deodorization) and metal or ions complexes (depollution or selective extraction of noble metals in the field. mining sector) [5].

Various researches have been devoted to the preparation and characterization of activated carbons from the ligno-cellulosic biomass of materials from different plant sources: rice straw [6-7], coconut shell [8], sorghum grains [9], date palm seed [10], almond shell [11], bean pod [12].

Activated carbon can be obtained either by chemical activation or by physical activation. The physical activation takes place in two stages and at high temperatures between 400-900 °C,

unlike the chemical activation which takes place at the same time as the carbonization under an inert atmosphere between 400 and 600 °C, after impregnation of the precursor by an activating agent such as phosphoric acid [13–14], zinc chloride [15], alkali carbonates [16], potassium hydroxide [17], and more recently sodium hydroxide [18]. The chemical activation is followed by the heat treatment step, and finally by a washing step to remove chemical agents and products of inorganic reactions [19].

The general objective of this work is to prepare activated carbon from *Raphia farinifera* fruit kernels, having a better porosity and important chemical property for the reduction of chromium (VI) in aqueous medium. As a specific objective, we will prepare activated carbons from *Raphia farinifera* fruit stones by chemical activation with phosphoric acid (H_3PO_4), characterize them and test the performance of activated carbons prepared for the removal of chromium (VI) in aqueous medium. The adsorption study consisted of discussing the effects of contact time and the pH of the solution using a batch adsorption technique. The effect of temperature made it possible to carry out a thermodynamic study to define the nature of the absorption phenomena. In addition, different kinetic models (first and second order and Intra-particle) and adsorption isotherms (Langmuir, Freundlich) were applied for the evaluation of the adsorption capacity.

MATERIALS AND METHODS

Preparation of activated carbon

The fruit kernels precursors of *Raffia farinifera* were harvested in the West Cameroon region, more precisely in the locality of Koupa Ngagnou (Foumban) located between 5.775256° North latitude and 10.88752 ° East longitude. The fruit kernels of *Raphia farinifera* were then crushed using a hand hammer. These precursors were washed thoroughly to remove all the stains and other impurities contained in the biomass and then dried under the sun for 20 days, in order to remove any water molecules contained in the biomass. On the other hand, they were grind using a hammer mill type grinder to obtain a powder. A particle size analysis (sieving) was carried out to retain the homogeneous fine particles characterized by a diameter of 63 µm.

However, the retained powder was impregnated with phosphoric acid (H_3PO_4) before carbonization. The method consists of mixing a mass of 20 g of *Raphia farinifera* fruit kernels powdered with a solution of the oxidant H_3PO_4-water. The resulting mixture was stirred

magnetically at room temperature for 2 hours and then heated in an oven at 110 °C to evaporate the water [20]. This was applied for different mass ratio called AC1/1, AC1/2 and AC1/3. In addition, the impregnate was introduced into a ceramic crucible and calcined in a NABERTHERM brand furnace at a maximum temperature of 470 °C with a rise rate of 5 °C / min and two hours of residence. After that, the activated carbon obtained was washed thoroughly with distilled water until neutralization of the rinsing water by regular checking of the pH = 7 in order to remove any carbonization residues and traces of activator, this made it possible to clean the microporosity of the activated carbon. Finally, the activated carbon was dried in an oven at 110 °C for 16 hours then recovered and stored in the flasks after cooling to room temperature.

Characterization of the powder and prepared activated carbon

Thermogravimetric, Differential Thermal and Differential Scanning Calorimetry (TG-DTG-DSC) analysis were performed to determine the ligno-cellulosic constituents (hemicellulose, cellulose and lignin) and the maximum carbonization temperature of the sifted powder of Raffia farinifera fruit kernels. The chemical functions present on the surface of the precursor material and the prepared activated carbon are determined by Fourier transform infrared (FT-IR). The sampling method consists of obtaining pellets by compressing the samples with potassium bromide (KBr). Samples were taken, scanning for wave numbers from 4000 to 400 cm^{-1}, using an FT-IR spectrometer.

Determination of the surface chemical functions of activated carbon by the Boehm method

The Boehm method makes it possible to identify and quantify basic groups and surface acids, and more precisely carboxylic (R – COOH), lactone (R – OCO), phenol (Ar – OH), carbonyl or quinone functional groups. (RR'C = O) [21]. Indeed, a mass of 0.1 g of each activated carbon was mixed with a volume of 50 mL of an aqueous solution of concentration 0.1 mol. L^{-1} of reagent sodium hydrogen carbonate ($NaHCO_3$, Pka = 6.3), sodium carbonate (Na_2CO_3, Pka = 10.2), sodium hydroxide (NaOH, pka = 15.7), sodium ethanoate ($NaOC_2H_5$, pKa = 20.5) and hydrochloric acid (HCl). The mixtures were stirred magnetically at room temperature for 10 hours. Then the suspensions were filtered through whatman brand filter paper. In order to quantify the oxygen-containing group content, a volume of 10 mL of the filtrate was titrated with an HCl solution of concentration 0.1 mol. L^{-1}. Whereas, the contents of the basic groups were

also determined by back titration of a volume of 10 mL of the filtrate with a NaOH solution of concentration 0.1 mol.L^{-1}. We did the volumetric assay (pH-metric) and the Hanna-type pH meter was used to measure the pH of the solution.

He number of moles of the function sought is given by the following formula:

$$n_{éqR} = N_iV_i - N_fV_f \quad (1)$$

With: $n_{éqR}$ being the number of gram equivalent reacted, N_iV_i the number of gram equivalent before the reaction and N_fV_f the number of gram equivalent after the reaction. The acidic or basic functions were determined by the following expression:

$$\text{Acid functions (meq g}^{-1}) = \frac{n_{éqR}}{m_{CA}} \times 100 \quad (2)$$

With: m_{AC}: mass of activated carbon

Contact pH

Measuring the contact pH makes it possible to quickly assess the acidity or basicity of activated carbon. Therefore, a mass of 0.1 g of activated carbon was brought into contact with an NaCl solution of concentration 0.1 mol.L^{-1} at pH = 6.8. The suspension was stirred at room temperature for 10 hours. The mixture was then filtered using whatman brand filter paper to measure the contact pH of our activated carbons.

pH at zero charge point

Six NaCl solutions with a concentration of 0.1 mol. L^{-1} with a pH of between 2 and 12 (adjusted by adding NaOH or HCl at 0.1 mol L^{-1}) were prepared and checked by a Hanna brand pH-meter beforehand. Subsequently, a volume of 50 mL of each of these solutions was contacted with a mass of 0.1 g of AC. The mixture was stirred magnetically at room temperature for 10 hours. Each sample was then filtered using whatman filter paper. Finally, the final pH was measured and plotted against the initial pH. In short, the pH_{PCN} is the point of intersection of the first bisector between the curve $pH_{final} = f(pH_{initial})$ [22].

Iodine number

The technique used here is that of the Duchet Study Center, which is an adaptation of the CEFIC 1989 method and of the AWWA B 600 - 78 standard. Indeed, a volume of 20 mL of the iodine solution (I_2) of normality 0.02 N was mixed with a mass of 0.1 g of activated carbon. The mixture was stirred at room temperature for 30 minutes. After that, 10 mL of the iodine filtrate in the presence of three drops of starch was titrated with 0.1 N sodium thiosulfate (Na_2SO_3). The iodine number I_2 (mg /g) can be calculated by the following formula:

$$Q_{I2} = \frac{\left(C_0 - \frac{C_n V_n}{2 V_{I_2}}\right) \times M_{I_2} V_{abs}}{m_{CA}} \quad (3)$$

With: V_n: the volume of sodium thiosulfate (mL), C_n: the concentration of sodium thiosulfate (0.1 mol/L), C_O: the concentration of the initial iodine solution (0.02 mol/L), V_{I2}: the volume of iodine assayed (10 mL), M_{I2}: the molar mass of iodine (253.81 g/mol), V_{abs}: the adsorption volume (20 mL) and m_{AC}: mass of the carbon active (0.1 g).

Knowing the amount of iodine adsorbed at equilibrium per gram of activated carbon (Q_e) leads to the determination of the specific surface area (S_{I2}) by applying the relationship:

$$S_{I2} = Q_e.\sigma\ N_A/MI_2\ (m^2.g^{-1}) = 1{,}28.10^5\ Q_e / MI_2\ (m^2.g^{-1}). \quad (4)$$

The area occupied by an iodine molecule is equal to σ = 21.3 Å^2 and N_A = 6,023.1023 mol^{-1} is the Avogadro number and the molar mass of iodine (M_{I2}) is 126.9 g. mol^{-1}.

Methylene blue number

A volume of 50 mL of a methylene blue solution with different initial concentrations: 100, 200, 400, 600, 800, and 1000 mg. L^{-1} was mixed with a mass of 0.1 g of activated carbon. The mixture was stirred magnetically at room temperature for 2 hours. The filtrate was assayed with a SCHOTT Instrument brand UV-Visible spectrophotometer at a maximum wavelength of 660 nm [23]. The adsorbed amount (Qe, mg. g^{-1}) of methylene blue is determined by the following formula:

$$Qe = \frac{C_0 - C_e}{m_{CA}} \text{ x } V \quad (5)$$

Where: C_o is the Initial Concentration of MB (mg. L^{-1}), this is the Concentration of MB in the equilibrium mixture (mg. L^{-1}), m_{AC} is the mass of the adsorbent (g) and V is the Volume of the solution containing the MB (mL).

The estimation of the specific surface area of an adsorbent is conventionally based on measurements of the adsorption capacity for a given solute. It just to determine the value of the adsorption capacity of the monolayer from the adsorption isotherm [24]. For the determination of the specific surface area S_{BM} (m^2. g^{-1}), we write the Langmuir equation in the following linear form:

$$\frac{1}{Q_e} = \frac{1}{K_L Q_{max} C_e} + \frac{1}{Q_{max}} \quad (6)$$

Where: Q_{max} is the theoretical maximum adsorption capacity (mg/g) and K_L is Langmuir equilibrium adsorption constant (L/mg). The parameters K_L and Q_{max} are determined from the plot $\frac{1}{Q_e} = f(\frac{1}{C_e})$.

The knowledge of Q_{max} leads to the determination of the specific surface S_{BM} by the relation:

$$S_{BM} = Q_{max}. A_m. N_A/M_{MB} \quad (7)$$

Where: S_{BM} is the specific surface area determined using MB as adsorbate (m^2/g); (A_m) is the air occupied by a MB molecule (175 $Å^2$), Q_{max} is the maximum adsorption capacity of MB (mg/g), N_A is the Avogadro number (6,023.1023 mol^{-1}) and M_{MB} is the molar mass of MB of (319.85 $g.mol^{-1}$).

Thus, the Langmuir constant K_L (L. mol^{-1}) makes it possible to determine the molar free energy of reaction ($\Delta G°$, J. mol^{-1}) from the following relationship:

$$\Delta G° = - RT \ln K_L \quad (8)$$

Where R is the ideal gas constant (J. mol^{-1}. K^{-1}) and T the temperature (°K).

Adsorption of chromium (VI) on prepared activated carbon

The adsorption of chromium (VI) on activated carbon was carried out as follows: a mass of 0.1 g of activated carbon was brought into contact with a volume of 30 mL of the chromium (VI)

solution at a good concentration defined. The mixture was stirred magnetically at room temperature for a well-defined time t then the filtrate assayed with a SCHOTT Instruments brand UV-Visible spectrophotometer at a maximum wavelength of 350 nm. The adsorption capacity (Qe, mg/g) of chromium (VI) is determined by relation (5) above.

Chromium (VI) adsorption kinetics on prepared activated carbon

Pseudo-first order, pseudo-second order and intra-particle diffusion models were tested to model the kinetics of chromium (VI) adsorption on prepared activated carbon.

Pseudo-first order kinetic model

The linear form of the pseudo-first order model is given by the following relation [25]:

$$\text{Ln}\,(Q_e - Q_t) = \text{Ln}\,(Q_e) - K_1\,t \qquad (9)$$

With: k_1 the rate constant for pseudo first order kinetics (min^{-1}), Q_t and Q_e the adsorption capacities at time t ($mg.g^{-1}$) and at equilibrium ($mg.g^{-1}$), respectively.

The constants of the model are determined graphically by plotting Ln (Q_e-Q_t) against t. Furthermore, the equilibrium adsorption half time ($t_{1/2}$, min) and the difference between the equilibrium adsorption capacities (Δq) are determined by the following equations:

$$t_{1/2} = \frac{Ln2}{K_1} = \frac{0{,}693}{K_1} \qquad (10)$$

$$\Delta q = \left| Q_{emax}\,(\text{exp}) - Q_e\,(\text{th}) \right| \qquad (11)$$

Where: Q_{emax} (exp) is the adsorption capacity obtained experimentally and Q_e (th) is the theoretical adsorption capacity deduced from the kinetic relationships.

Pseudo-second order kinetic model

The linear form of the pseudo-second order model is described by the following equation [26]:

$$\frac{t}{Q_t} = \frac{1}{K_2 Q_e^2} + \frac{1}{Q_e}\,t \qquad (12)$$

Where: k_2 is the rate constant for second order kinetics (g.m$g^{-1}.min^{-1}$) Q_t and Q_e: The adsorption capacities at time t (mg .g^{-1}) and at equilibrium (mg.g^{-1}), respectively. The adsorption kinetic rate constant K_2 as well as the amount of solute adsorbed at equilibrium Q_e are determined experimentally from the plot of $t/Q_e = f(t)$. Thus, the half-adsorption time ($t_{1/2}$), min), the difference (Δq) (equation 11) and the initial adsorption rate (h) in (mg.$g^{-1}min^{-1}$) are obtained from the following relations:

$$t_{1/2} = \frac{1}{K_2 Q_e (th)} \quad (13)$$

$$h = K_2.Q_e^2 (th) \quad (14)$$

Kinetic model of intra-particle diffusion

The linear model of intra-particulate diffusion is given by the following equation [27]:

$$Q_t = K_d \times t^{1/2} + I \quad (15)$$

Where: K_d is the intra-particulate diffusion rate constant (mg.$g^{-1}.min^{-1/2}$) and I is the constant related to the thickness of the boundary layer (mg/g).

The representation of Q_t as a function of ($t^{1/2}$) makes it possible to calculate K_d, I and to highlight the different stages of the adsorption process.

Chromium (VI) adsorption isotherms on prepared activated carbon

Langmuir and Freundlich models were applied to model chromium (VI) adsorption isotherms on prepared activated carbon.

Langmuir model

The linear form of the Langmuir isotherm is described by the following equation [28]:

$$\frac{1}{Q_e} = \frac{1}{K_L Q_{max} C_e} + \frac{1}{Q_{max}} \quad (16)$$

Where: C_e is the Concentration of chromium (VI) at equilibrium (mg. L^{-1}), Qe is the amount of chromium (VI) adsorbed per mass unit of adsorbent (mg/g), Q_{max} is the capacity maximum

theoretical adsorption (mg. g^{-1}) and K_L is the Langmuir constant of the adsorption equilibrium (L. mg^{-1}). The parameters are determined from the plot of $\frac{1}{Q_e}$ = f ($\frac{1}{C_e}$).

Freundlich model

The linear form of the Freundlich isotherm is given by the following expression [29]:

$$\text{Ln } (Q_e) = \ln (K_F) + \frac{1}{n_f} \ln (C_e) \quad (17)$$

Where: n_f is the constant indicating the adsorption intensity, C_e is the Concentration of the solute at equilibrium (mg. L^{-1}) and K_f is the constant relating to the adsorption capacity of the adsorbent (Freundlich Constant) ($mg^{1-(\frac{1}{n})}.L^{1/n}.g^{-1}$).

The parameters K_f and n_f are determined from the graphical representation of

$$\text{Ln } (Q_e) = f (\ln (C_e)).$$

Thermodynamic aspects of chromium (VI) adsorption on activated carbon

The thermodynamic parameters such as: variation of free energy (ΔG°), free enthalpy (ΔH°) and entropy (ΔS°) were determined from the following equations [30]:

$$\Delta G° = \Delta H° - T\Delta S° \quad (18)$$

$$\text{Ln } K_d = -\frac{\Delta H°}{RT} + \frac{\Delta S°}{R} \quad (19)$$

$$K_d = \frac{Q_e}{C_e} \quad (20)$$

Where: ΔG° is the varition in free energy (kJ. mol^{-1}), ΔH° is the variation in free enthalpy (kJ. mol^{-1}), ΔS° is the variation in entropy (k^{-1}. J. mol^{-1}), R is the ideal gas constant (8.314 J. mol^{-1}. K^{-1}), T is the absolute temperature (°K), it is the concentration of chromium (VI) at equilibrium (mg.L^{-1}) and Q_e is the adsorption capacity of chromium (VI) at equilibrium (mg. g^{-1}).

The values of ΔH° and ΔS° were determined from the plot of Ln (K_d) = f (1/T).

RESULTS AND DISCUSSION

Characterization of powder and activated carbons prepared from *Raffia farinifera* fruit kernels

Thermogravimetric analysis

Figure n_0.1 show the thermogram of the *Raffia farinifera* fruit kernels coupled to TG/DTG/DSC.

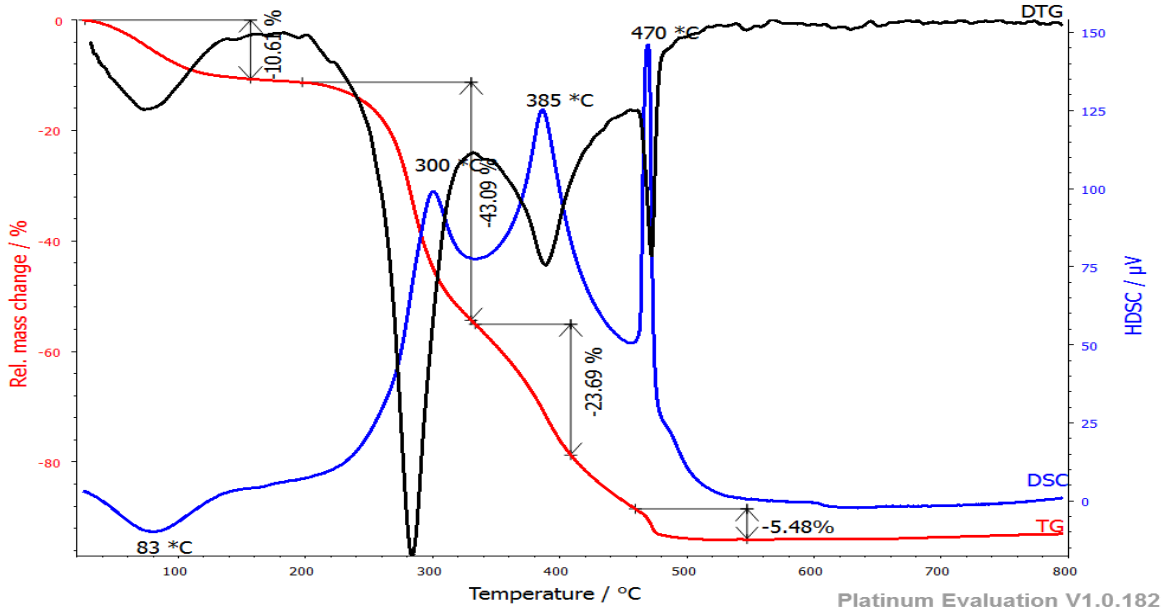

Figure No. 1: Thermogram of the *Raffia farinifera* fruit kernels powder coupled with TG/DTG/DSC

It follows, from the coupled TG/DTG/DSC analysis of the *Raffia farinifera* fruit kernels powder that the thermogram is subdivided into four stages: the first 10.6 % mass loss marked by an endothermic peak around 83 °C could be due to the dehydration reaction. This is due to the departure of humidity from the biomass, as well as free water molecules. The second loss of mass at 43.09 % marked by an exothermic peak around 300 °C could be attributed to the degradation of the hemicelluloses. This could be justified by the fact that hemicelluloses are formed of small molecules, more sensitive to heat and which produce less tar and the most non-condensable gases such as CO and CO_2. Then, the third mass loss at 23.69 % marked by an exothermic peak around 385 °C could be that of the thermal decomposition of cellulose,

characterized by the release of abundant gas rich in CO and CO_2. Finally, the fourth 5.48 % mass loss manifested by an exothermic peak around 470 °C could be the thermal decomposition of lignin. This could be due to the breaking of C-O-C bonds (ethers) and C-C bonds which have low energy.

In general, the decomposition of hemicelluloses occurs between 200 and 300 °C, that of cellulose between 300 and 400 °C and that of lignin in a wider range, between 250 and 500 °C [31].

We can therefore conclude that our material: *Raffia farinifera* fruit kernels, contains hemicellulose, cellulose and lignin thus confirming the lignocellulosic structure. Moreover, this analysis allowed us to determine the maximum calcination temperature around 470°C. Beyond this temperature we observe a stability on the thermogram which means that all the cellulose has decomposed as well as all the hemicelluloses.

Analysis of the FTIR spectra obtained

The FTIR spectra of powder and activated carbons prepared from recorded *Raffia farinifera* fruit kernels are shown in Figure n$_{0.}$ 2 below.

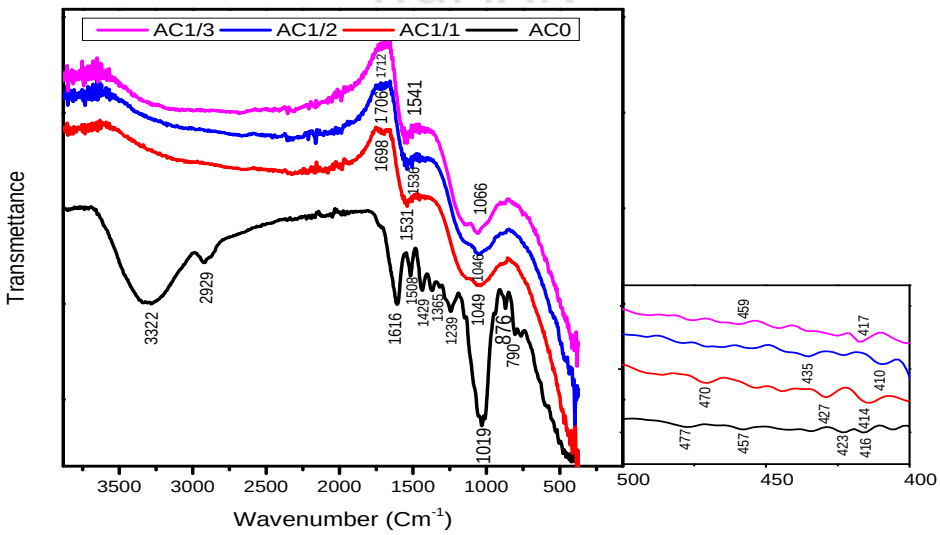

Figure No. 2: FTIR spectra of *Raffia farinifera* fruit kernels powder and prepared activated carbons

The treatment of *Raffia farinifera* fruit kernels powder by impregnation with phosphoric acid and calcination causes a modification (appearance and disappearance) on the structure of the precursor material. Indeed, the peak at 3322 cm^{-1} observed on the AC_0, which corresponds to the valence vibration of the O-H bonds, undergoes a strong decrease in intensity until complete disappearance after impregnation and calcination. As this peak corresponds to all hydroxyls, primary and secondary, the disappearance of the band can be explained by the conversion to carboxylic acid of part of the primary alcohols and the thermal decomposition of the chemisorbed water. The peak at 2929 cm^{-1} observed on the AC_0 which corresponds to the C-H elongation vibrations of the cellulose has undergone a significant change after treatment with phosphoric acid, the content of which decreases until complete disappearance since the cellulose degrades between 300 and 400 °C before the maximum calcination temperature (470 °C). It follows the characteristic peaks of 1712 to 1616 cm^{-1} which can be attributed to the elongation vibrations of C=O of ketones, aldehydes, lactones or carboxyl groups or C=N of amines and O-H of water. This peak, which is related to the ester functions of hemicelluloses, gradually decreases after modification of the *Raffia farinifera* fruit stones. This suggests that the hemicellulose content has decreased and the shift towards the large absorption bands is probably due to the effect of H_3PO_4 on the structure of the biomass [32]. The absorption peaks observed at 1541-1508 cm^{-1} correspond to the stretching of the aromatic ring of the C=C bonds in the line of the aromatic ring of lignin. It remains changed after treatment with phosphoric acid. The peaks at 1429 and 1365 cm^{-1} observed on AC_0 which correspond to the deformation in the plane of C-H groups and aromatic vibration of hemicellulose, cellulose and lignin. Likewise, the peak at 1239 cm^{-1} which corresponds to the C-O elongation of the acetyl groups of the C-O lignin of the aromatic ring of cellulose disappeared after treatment [33]. An intense band at 1066-1019 cm^{-1} on AC_0, AC1/1, AC1/2 and AC1/3 corresponds to the extremity of the stretching modes of the hydroxyl and ether groups C-O or aromatic deformation in the C-H plane and Si-O-C elongation, these peaks are characteristic of the absorption of cellulose and hemicellulose and changed (decrease in intensity and shift of bands towards long wavelengths) after impregnation and calcination of *Raffia farinifera* fruit kernels. The peak at 876 cm^{-1} corresponds to the C-H elongation vibrations of cellulose and underwent significant change after treatment with phosphoric acid. The absorption band at 790 observed on AC_0 can be attributed to the NH_2 strain. The peaks between 477 to 410 cm^{-1} can be attributed to the elongation vibrations: C-F, C-

Cl, C-Br and S-S. We find that phosphoric acid altered the structure of *Raffia farinifera* fruit kernels. We have identified a number of the structures such as: C-H, O-H, C=O, C = N, C=C, C-O, NH_2 and C-O-C. The presence of lignin, hemicellulose, and cellulose in the matrix of *Raffia farinifera* fruit kernels of (AC_0) confirms the lignocellulosic constituents obtained at TG.

Surface chemical functions, pH at zero charge point and contact pH

The experimental results obtained are shown in Table n_0. 1 and the principle of determining the pH at the point of zero charge (pH_{PCN}) in Figure n_0.3.

Table No. 1: Surface chemical functions, pH at zero charge point and contact pH

Activated carbon	AC1/1	AC1/2	AC1/3
-COOH (carboxyls) meq. g^{-1}	0,55	0,53	0,45
-COO- (lactones) meq. g^{-1}	0,26	0,09	0,11
-OH (phenols) meq. g^{-1}	0,58	0,55	0,59
-CO (carbonyls) meq. g^{-1}	0,45	0,50	0,51
Total acid group meq. g^{-1}	1,84	1,67	1,66
Total basic group meq. g^{-1}	0,15	0,26	0,06
Character	Acid	Acid	Acid
pH_{PCN}	5,63	5,83	5,66
contact pH	5,7	5,3	5,4

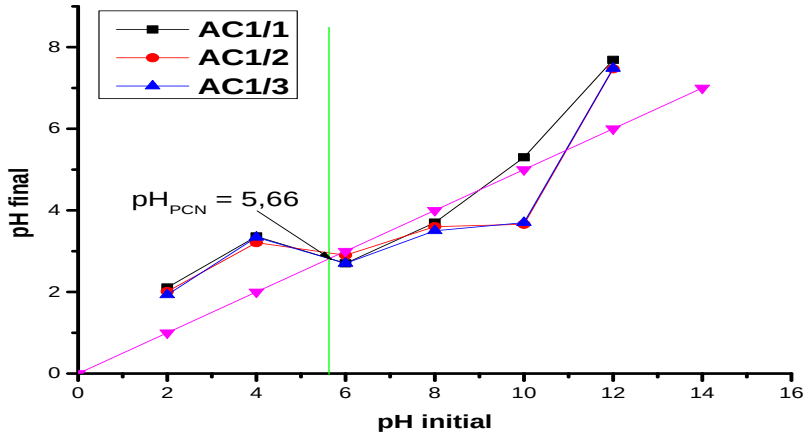

Figure No. 3: Principle of determination the pH at zero charge point (pH_{PCN})

The first remark of Table 1 is the consistency of the pH_{PCN} and contact pH values with respect to the proportions in acid and basic functions.

As far as concerned the surface chemical functions, the results listed in Table n_0. 1 show that the contents of the acid functions are much greater than those of the basic functions. The contents of the acid functions could be justified by the presence of phenol, carboxyl, carbonyl and lactone groups. On the other hand, the basic contents could be justified by the presence of pyrones, aromatic C_π groups and basic mineral oxides. The surface functions of activated carbon are acidic in nature. These results suggest that the prepared activated carbons would have a high degree of adsorption [34]. Our prepared activated carbons, although they are predominantly acidic, have basic functions on their surfaces, which gives them double reactivity with respect to the chemical nature of the pollutant (cationic or anionic) to be treated.

However, the pH_{PCN} obtained for each AC in Table n_0. 1 is consistent with the quantification of the surface functional groups obtained by the Boehm method. It emerges from Table 1 that all the activated carbons prepared have an acidic character (pH_{PCN} = 5.6, 5.83 and 5.66), respectively for AC1/1, AC1/2 and AC1/3. This could be attributed by the contents of carboxylic acid groups, phenols, lactones and carbonyls present in the material. Indeed, Lopez-Ramon agree in concluding that there is a decrease in pH_{PCN} when the oxygen content of the activated carbons increases, which would tend to confirm that the basicity of the carbons is rather linked to the sites rich in π electrons, than to oxygenated surface functions [22]. Furthermore, the adsorption of cationic species is favored at pH > pH_{PCN} and anionic adsorption is favored at pH < pH_{PCN} because the surface charge is generally positive at pH < pH_{PCN} and overall negative at pH > pH_{PCN}. Therefore, for manipulations at pH = 2 all ACs will have their positively charged surface (pH_{PCN} > pH) while at (pH_{PCN} < pH) they will have a negatively charged surface. This can be of great importance in the interactions between molecules/adsorbent material in the liquid phase. This could explain the high adsorption capacity of chromium (VI) at pH = 2 in aqueous medium.

However, the contact pH obtained for each AC in Table 1 is consistent with the quantification of the surface functional groups obtained by the Boehm method and the pH_{PCN}. The decrease in pH (from 6.8 to 5.7, 5.3 and 5.4), respectively for AC1/1, AC1/2 and AC1/3 could be due to the presence of the contents of carboxyl groups, phenols, lactones and carbonyls present in the material as well as the strong oxidant (H_3PO_4) used as the activator.

Iodine and methylene blue number

The experimental results of the iodine number and methylene blue adsorption test on the prepared activated carbons are shown in Table n_0.2 and the adsorption isotherm in Figure 4 below.

Table No. 2: Results of iodine and methylene blue number

Activated carbon	AC1/1	AC1/2	AC1/3
Methylene blue number (I_{MB}, mg. g^{-1})	322,580	344,830	476,190
Specific surface area (S_{MB}, m^2. g^{-1})	1063,740	1136,120	1568,920
Separation factor (RL. 10^{-4})	8,440	9,840	6,790
Langmuir constant (K_L, L. mg^{-1})	2,818	2,417	3,500
Free energy ($\Delta G°$, J. mol^{-1})	-28852,483	-29232,982	-28315,235
Iodine number (Q_{I2}, mg. g^{-1})	913,716	939,097	964,478
Specific surface area (S_{I2}, m^2. g^{-1})	923,724	949,383	975,042

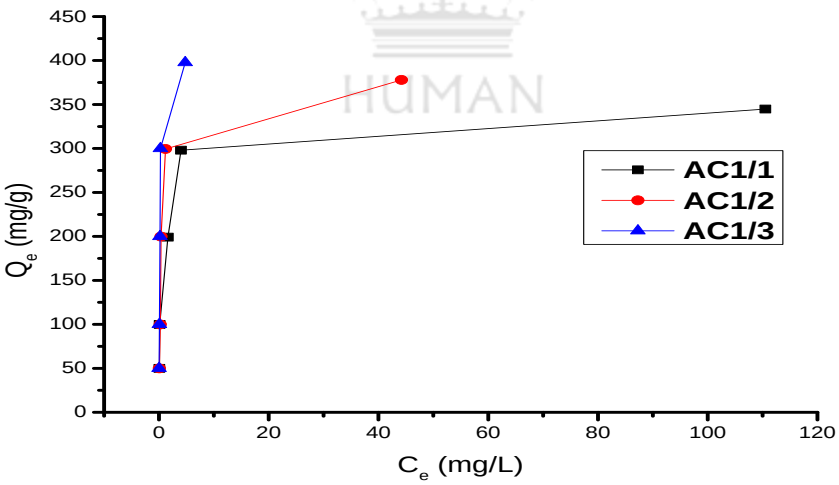

Figure No. 4: Methylene blue adsorption isotherm on activated carbon: Experimental conditions (m_{AC} = 0.1 g, V = 50 mL, t = 2 h, T = 25 ± 2 °C)

For the methylene blue number, Figure 4 shows the adsorption isotherm of methylene blue on the prepared activated carbon. We find that the adsorption capacity gradually increases with increasing concentration and the plateau is not clearly reached indicating a wide distribution of

heterogeneous microporosity and well-developed mesoporosity. Therefore, the AC1/1, AC1/2 and AC1/3 isotherm obtained will be of type (I_C) [35]. Moreover, the values of the adsorption capacity of MB (Q_{max} = 322.58, 344.83 and 476.19 mg/g), respectively for AC1/1, AC1/2 and AC1/3, increase with the ratio impregnation mass, indicate better mesoporosity. In addition, the values of the specific surface of methylene blue (S_{MB} = 1063.74, 1136.12 and 1568.92 $m^2. g^{-1}$), show that these activated carbons have very large exchange surfaces, for AC1/1, AC1/2 and AC1/3, respectively. By comparing these values with those found in the literature (300-1500 $m^2. g^{-1}$) we can say that our activated carbons comply with the standards for the specific surface area of activated carbons and this justifies their good adsorbing power [36]. Thus, the values of the dimensionless separation factor (R_L = 8.44, 9.84 and 6.79. 10^{-4}) tend towards 0, which indicates that the conditions of adsorption of methylene blue on our prepared activated carbon are favorable. In addition, negative values of free energy ($\Delta G°$) indicate the feasibility and spontaneity of the adsorption process, which is thermodynamically favorable and thus confirms the affinity of methylene blue on all the activated carbons prepared.

However, the iodine value results presented in Table n_0.2 show that the concentration of phosphoric acid influences the structure of *Raffia farinifera* fruit kernels. Therefore, increasing the concentration of phosphoric acid promotes the increase in the iodine number of activated carbon (Q_{I2} = 913.716, 939.097 and 964.478 mg. g^{-1}) for AC1/1, AC1/2 and AC1/3, respectively [37]. By comparing these values with those found in the literature (550 mg. g^{-1}) we can say that our activated carbons are more microporous and comply with the standards for iodine numbers of activated carbons and this could justify their good adsorbing power [20]. Furthermore, the values of the specific surface area of iodine (S_{I2} = 923.724, 949.383 and 975.042 $m^2. g^{-1}$), show that these activated carbons have very large exchange surfaces for AC1/1, AC1/2 and AC1/3, respectively. It appears that all our prepared activated carbons have their high iodine numbers as well as their specific surfaces and therefore are more likely to adsorb small molecules (iodine) such as those which are responsible for tastes and odors [38].

By comparing, the results of the iodine and methylene blue value as well as their specific surface area obtained with those found by [39]. We can say that the mass ratio AC1/1, AC1/2 and AC1/3 could be relatively indicated for the preparation of good quality activated carbons as well as for the depollution of organic and inorganic compounds in aqueous medium.

Batch adsorption study

Chromium (VI) adsorption kinetics on activated carbon

Figure n_0. 5 shows the experimental results of chromium (VI) adsorption on all activated carbons.

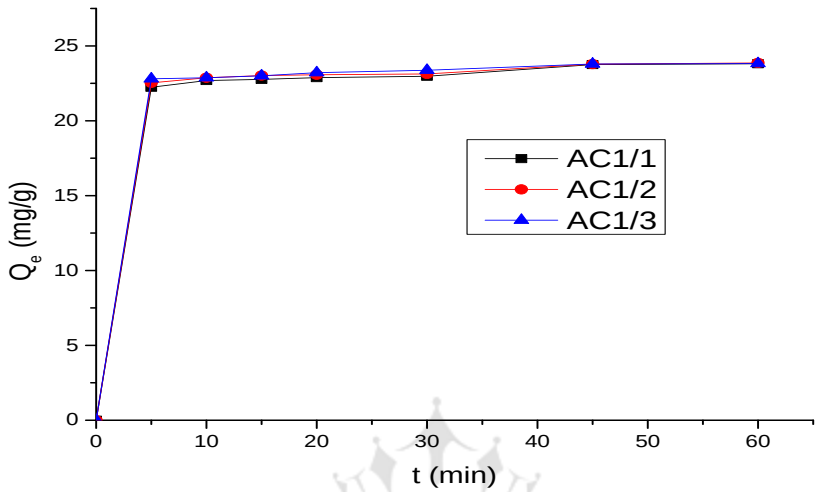

Figure No. 5: Influence of the contact time of chromium (VI) on activated carbon: experimental conditions (m_{AC} = 0.1 g, V = 30 mL, C = 80 mg. L^{-1}, T = 25 ± 2 °C and pH = 2)

Figure 5 shows a first significant chromium (VI) adsorption phase during the first 10 minutes at the end of which 22.694 for AC1/1 and 22.871 for AC1/2 and AC1/3 mg of chromium (VI) per gram of carbon active are adsorbed. This is characterized by the high affinity of the activated carbon for the retention of chromium (VI) and by better diffusion (external mass transfer) of the substrate through the pores of the AC. This increase could be due to the large number of vacant sites available on the surface of the AC used [40]. Then we observed a second phase corresponding to a long phase (from 15 to 60 minutes) where the adsorption capacity increases slightly (23.806, 23.861 and 23.824 mg. g^{-1}) for AC1/1, AC1/2 and AC1/3, respectively, until reaching a plateau which reflects the final state of equilibrium, due to the fact that the intra-particulate diffusion tends to cancel out, in other words, all the adsorption sites become occupied in the presence of a high chromium (VI) content [41]. On this basis, for the rest of our study, the optimal time will be 60 minutes.

The mathematical models of pseudo first and second order and intra-particulate diffusion have been applied to describe the adsorption of chromium (VI) to activated carbon. The experimental results obtained are compiled in Table n_0. 3 and the curves of the kinetic model of intra-particulate diffusion in figure n_0. 6 below.

Table No. 3: Constants of the kinetic models of adsorption of chromium (VI) on activated carbon and correlation coefficient (R^2)

Models	**Parameters**	**AC1/1**	**AC1/2**	**AC1/3**
Pseudo-first order	R^2	0,795	0,817	0,852
	K_1 (min^{-1})	0,075	0,062	0,081
	Q_e (th) (mg. g^{-1})	3,112	2,220	2,397
	Q_{emax} (exp) (mg. g^{-1})	23,806	23,862	23,824
	Δq	20,694	21,642	21,426
	$t_{1/2}$ (min)	9,267	11,216	8,589
Pseudo-second order	R^2	1,000	1,000	0,999
	K_2 (g. mg^{-1}. min^{-1})	0,394	0,504	0,327
	Q_e (th) (mg. g^{-1})	22,990	23,150	23,360
	Q_{emax} (exp) (mg. g^{-1})	23,806	23,862	23,824
	Δq	0,816	0,712	0,464
	h (mg. g^{-1}. min^{-1})	208,245	270,100	178,440
	$t^{1/2}$ (min)	0,11	0,085	0,13
Intra- diffusion Particulate	R^2	0,940	0,944	0,968
	K_{id} ((mg. g^{-1}).$min^{-1/2}$)	0,284	0,238	0,210
	I (mg. g^{-1})	21,640	22,039	22,256

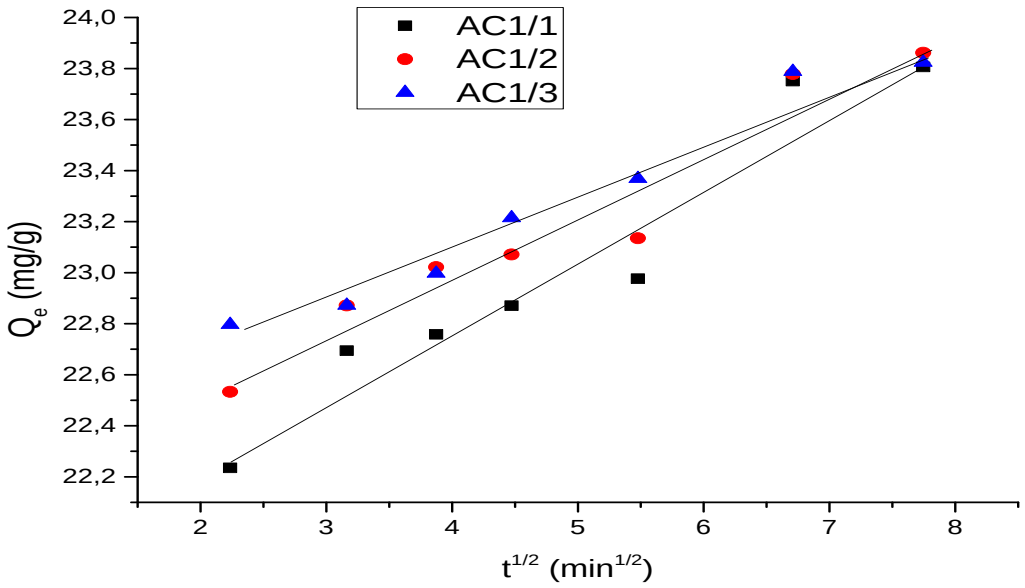

Figure No. 6: Kinetic model of intra-particulate diffusion of chromium (VI) on activated carbon: experimental conditions (m_{AC} = 0.1 g, V = 30 mL, C = 80 mg. L^{-1}, T = 25 ± 2 °C and pH =2)

According to the pseudo-first order model, we noticed from Table n_0.3 that, the correlation coefficients are not satisfactory ($R^2 \leq 0.852$), which indicates a bad correlation, a large relative deviation ($\Delta q \geq 20.614$) which indicates the non-conformity of the experimental and theoretical values, the kinetic rate constant is low ($K_1 \leq 0.081$ min^{-1}) and the half-adsorption time is large ($t_{1/2} \geq 8.589$ min). Therefore, the pseudo-first order model does not better describe the adsorption of chromium (VI) to activated carbons prepared from Raffia farinifera fruit kernels.

Regarding the pseudo-second order model, the results obtained show a perfect linearity of the regression lines of our prepared activated carbons, the correlation coefficients are much better ($R^2 \geq 0.999$ for AC1/3 very- very close of unity and $R^2 = 1$ for AC1/1 and AC1/2, the different deviations are small ($\Delta q \geq 0.816$), which justifies the conformity between the experimental and theoretical values. We notice that the increase in the values of ($K_2 \leq 0327$ g. mg^{-1}. min^{-1}) is consistent with the increase in adsorption capacity as well as the initial adsorption rate ($h \geq$ 178,440 mg. g^{-1}. min^{-1}) and time of half-adsorption is low ($t_{1/2} \leq 0.13$ min). The three activated carbons used are in decreasing order according to the sequence: AC1/2 > AC1/1 > AC1/3. In view of all the above, we can therefore conclude that the pseudo-second order model better describes the adsorption of chromium (VI) on all the activated carbons prepared.

Regarding the intra-particulate diffusion model, Figure n₀. 6 above clearly shows that not all the drawn lines go through the origin, the values of I large ($I \leq 21.640$), and the correlation coefficients are quite significant ($R^2 \leq 0.968$), these indicate that diffusion in the pores is involved in the sorption process but is not the only mechanism limiting the adsorption kinetics and it appears that the mechanism of extra diffusion particulate is also involved. The greater I, the greater the thickness of the diffusion boundary layer. Therefore, the adsorption capacity of chromium (VI) and the intra-particle constant decreases on activated carbon.

Chromium (VI) adsorption isotherms on activated carbon

The chromium (VI) adsorption isotherms on the three activated carbons are shown in Figure n₀. 7 below.

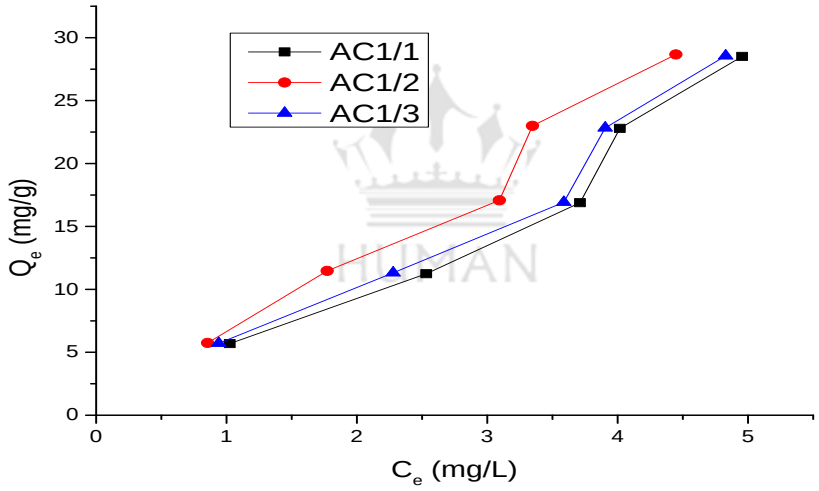

Figure No. 7: Chromium (VI) adsorption isotherm on activated carbon: experimental conditions (m_{AC} = 0.1 g, V = 30 mL, t = 1 h, T = 25 ± 2 °C and pH = 2)

The adsorption isotherms show that the quantity of chromium (VI) adsorbed on the activated carbons, Q_e (mg. g^{-1}), gradually increases with the increase in the initial chromium (VI) concentration and without clearly reaching the plateau for all three ACs used. This is justified by the unsaturation of the active sites on the surface of the AC. Indeed, the increase in the quantity adsorbed as a function of the initial concentration is due to the fact that in the presence of a high

concentration of chromium (VI), the forces of diffusion of the solute towards the activated carbon become markedly higher this which favors intra-particle diffusion phenomena [42].

The description of the adsorption isotherms was carried out by applying the models of Langmuir and Freundlich. The results of the characteristic parameters of the chromium (VI) adsorption isotherms on the prepared activated carbons are summarized in Table n_0.4 below.

Table No. 4: Characteristic parameters of chromium (VI) adsorption isotherms on activated carbon and correlation coefficient (R^2)

Models	**Parameters**	**AC1/1**	**AC1/2**	**AC1/3**
Langmuir	R^2	0,978	0,994	0,983
	Q_{max} (mg/g)	147,060	217,390	109,890
	K_L (L.mg^{-1})	0,039	0,032	0,057
	R_L	0,299	0,342	0,266
	$\Delta G°$ (kJ.mol^{-1})	-39,255	-39,745	-38,314
Freundlich	R^2	0,961	0,983	0,969
	K_f ($mg^{1-(\frac{1}{n})}.L^{1/n}.g^{-1}$)	5,150	6,590	5,700
	n_f	0,998	1,039	1,040
	$1/n_f$	1,002	0,963	0,960

Regarding the Langmuir model, Table n_0.4 gives the satisfactory values of the correlation coefficients ($R^2 \leq 0.978$) and maximum capacity ($Q_{max} \leq 109.890$ mg. g^{-1}) of chromium (VI) adsorption on all activated carbons. Thus, the values of R_L (0.299, 0342 and 0.266), respectively for AC1/1, AC1/2 and AC1/3, these values are between 0 and 1; which indicates that the chromium (VI) adsorption process on all three activated carbons would be favorable. In addition, negative values of free energy (ΔG°), indicate the feasibility and spontaneity of the adsorption process, thermodynamically favorable and thus confirms the affinity of chromium (VI) on all prepared activated carbons. The values of free energy (ΔG°), are low (-39,255, -39,745 and -383.314 kJ.mol^{-1}), respectively for AC1/1, AC1/2 and AC1/3. Consequently, the low energy of adsorption is characteristic of a physical adsorption of chromium (VI) on all activated carbons studied [43]. These results were confirmed by the thermodynamic study. Looking at all of the

above, we can therefore conclude that the Langmuir model better describes the adsorption of chromium (VI) on all the activated carbons prepared.

According to the Freundlich model, Table 4 gives the satisfactory values of the correlation coefficients ($R^2 \leq 0.961$) of the adsorption of chromium (VI) on all activated carbons. The values of K_f (5.150, 6.590 and 5.700 $mg^{1-(\frac{1}{n})}.L^{1/n}.g^{-1}$), for AC1/1, AC1/2 and AC1/3, respectively, show a high adsorption capacity and a good affinity of chromium (VI) on all the activated carbons. The descending order is as follows: AC1/2 > AC1/1 > AC1/3 this could be due to the position and shape of the pores of the activated carbon because, the microporosity, mesoporosity and specific surface area increase with the impregnation ratio. It is well noted that, the closer the value of n_f is to 1, the more the surface is homogeneous, which means that all the exchange sites have almost the same affinity for chromium (VI) and $1/n_f < 0$ indicates that adsorption is favorable [44]. We can therefore say that the Freundlich model better describes the adsorption of chromium (VI) on prepared activated carbons.

However, the Langmuir and Freundlich models better describe the adsorption of chromium (VI) to all activated carbons in the following descending order: AC1/2 > AC1/1 > AC1/3.

Influence of the pH of the solution

The experimental results obtained are shown in Figure n_0. 8 below.

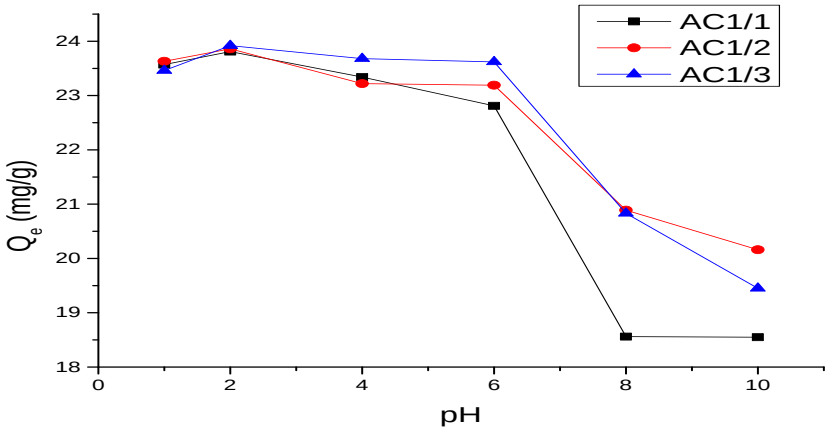

Figure No. 8: Influence of the pH of the chromium (VI) solution on activated carbon: experimental conditions (m_{CA} = 0.1 g, V = 30 mL, t = 1 h, C = 80 mg. L^{-1} and T = 25 ± 2 °C)

It emerges clearly in Figure 8 that the adsorption capacity of chromium (VI) on AC is high for low values of pH = 2: (Q_{emax} = 23.811, 23.865 and 23.919 mg. g^{-1}) for AC1/1, AC1/2 and AC1/3, respectively. This phenomenon confirms that the pH of the solution is an important factor that strongly affects the adsorption of metal ions and organic compounds to the surface of activated carbon. On the one hand, it affects the solubility of these ions and their speciation in aqueous solution and on the other hand, it controls the overall surface charge of activated carbon [45]. Indeed, activated carbons are materials of an amphoteric nature [45]. Their surfaces can be positively or negatively charged depending on the pH of the solution which governs the acid-base balances of the many surface functional groups located on the porous walls of the activated carbons. However, the analysis of pH_{PCN} (Table 1) reveals that the three activated carbons AC1/1 (pH_{PCN} = 5.63), AC1/2 (pH_{PCN} = 5.83) and AC1/3 (pH_{PCN} = 5.66) have an acidic character and the analysis of chemical function by Boehm titration thus confirms their predominantly acidic character but also weakly basic, which implies the presence of acidic surface functions (-OH, -C = O, -COO-, -COOH and NH_2) thus confirmed by FTIR analysis.

Therefore, the decrease in chromium (VI) adsorption capacity with increasing pH can be explained by the fact that the further away from pH_{PCN} towards lower pH values, the higher the positive charge density the surface of the carbon increases and therefore promotes electrostatic interactions between chromium ions ($HCrO_4^-$, CrO_4^{2-}) and the surface of activated carbon. In other words, as the number of H^+ ions increases with the lowering of the pH of the solution, this neutralizes the negative charge on the surface of the activated carbon and therefore limits the electrostatic repulsion of the ions and promotes their adsorption to the surface of the AC. The dominant form of chromate ions at pH = 2 is $HCrO_4^-$, which is therefore the form of hexavalent chromium adsorbed on the surface of activated carbon at this pH. On the other hand, the decrease in the adsorption capacity of chromium (VI) with the increase in pH may be due to the increase in the negative charge density at the surface of the ACs as well as to the increase in the number of OH^- ions in solution which compete with chromate and hydrogen chromate ions for adsorption. These observations suggest that the adsorption of hexavalent chromium ions on activated carbon involves chemisorption phenomena, involving valence forces through the sharing or exchange of electrons between the surface of the activated carbon and the ions, which is generally the case for the adsorption of metal ions on activated carbon [46]. Based on these

results, a pH = 2 was taken as the optimum value for the remainder of the study. This optimal value was also found [45].

Thermodynamic aspects of chromium (VI) on activated carbon

The experimental results obtained are summarized in Table n_0. 5 below.

Table No. 5: Thermodynamic parameters ΔG°, ΔH°, ΔS° relating to the adsorption of chromium (VI) on activated carbon and correlation coefficient (R^2)

AC	Temperature (°K)	$\Delta G°\ (KJ/mol)$	$\Delta H°$ (KJ/mol)	$\Delta S°(J.mol^{-1}.K^{-1})$	R^2
AC1/1	303,150	-11,380	-35,580	-79,82	0,978
	313,150	-10,580			
	323,150	-9,790			
	333,150	-8,990			
	343,150	-8,190			
AC1/2	303,150	-12,400	-38,530	-86,210	0,997
	313,150	-11,530			
	323,150	-10,670			
	333,150	-9,810			
	343,150	-8,950			
AC1/3	303,150	-11,140	-30,990	-65,490	0,989
	313,150	-10,480			
	323,150	-9,830			
	333,150	-9,170			
	343,150	-8,520			

Negative free energy values (ΔG°) indicate the feasibility and spontaneity of the chromium (VI) adsorption process on all activated carbon; increasing these values with increasing temperature indicates that adsorption occurs better at lower temperatures [47]. The values of ΔG° are more negative in the case of AC1/2, indicating an easy adsorption process. Thus, the negative values

of ΔH° and ΔS° (Table 5) again confirm that whatever the activated carbon considered here for the removal of chromium (VI), the adsorption process is spontaneous at low temperature and that the exothermicity is important. On the other hand, the change in entropy ΔS° is negative and indicates an increase in order. This suggests that adsorption causes an increase in order and that chromium (VI) molecules at the solid-liquid interface are more organized than those in the liquid phase. However physical and chemical adsorption can be classified, to some extent, by the magnitude of the enthalpy change. It is accepted that the bond strengths of ($\Delta H° < 82$ kJ mol^{-1}) are typically those of physical adsorption-type bonds. Chemisorption binding forces can vary from ($\Delta H° = 84$ to 420 kJ mol^{-1}) [48]. Based on this, the adsorption of chromium (VI) to all activated carbons appears to be a physical adsorption process.

CONCLUSION

The objective of this work is to prepare activated carbon from *Raphia farinifera* fruit kernels, having a better porosity and important chemical property for the reduction of chromium (VI) in aqueous medium.

Analysis of the TG curve results in the presence of hemicellulose, cellulose and lignin thus confirming the lignocellulosic structure. The surface of three activated carbons could be mainly acidic but also weakly basic with regard to pH_{PCN}, analysis of surface chemical function by Boehm and FT-IR titration (-OH, $-NH_2$, C=O –COO- and –COOH). These exhibit microporosity and mesoporosity on their surfaces. The value: of pH_{PCN} (5.6, 5.83 and 5.66) present an acidic surface, of the iodine number I_2 (913.716, 939.097 and 964.478 mg. g^{-1}) indicates a better microposity, of the I_{MB} methylene blue number (322.58, 344.83 and 476.19 mg. g^{-1}) justifies a better mesoporosity and specific surface area of methylene blue (S_{MB} = 1063.74, 1136.12 and 1568. 92 m^2. g^{-1}) shows a very large exchange surface of AC1/1, AC1/2 and AC1/3, respectively. The pseudo-second order kinetic model best describes the adsorption of chromium (VI) on AC, with $R^2 = 1$ for AC1/1 and AC1/2 and $R^2 = 0.9996$ for AC1/3. The Langmuir and Freundlich model better describes the adsorption of chromium (VI) on AC, with $R_L \leq 0.342$ and $K_f \geq 5.150$. The thermodynamic study gave the negative values of the free energy which justify the feasibility and the spontaneous nature of the process of adsorption of chromium (VI) on AC, the negative values of the free enthalpy and the entropy translate that the adsorption process is exothermic and indicates an increase in order at the solid/liquid interface. The low values of the

free enthalpy ($\Delta H° < 0$ kJ mol^{-1}) indicate that the chromium (VI) adsorption process on all ACs is physical.

Acknowledgment

The authors thank the "Labo Matgenie" for their granulometry equipment and the "Mipromalo" for their calcination equipment.

REFERENCES

[1] Richardson SD. Environmental Mass Spectrometry: Emerging contaminants and current issues Analytical Chemistry. 2012; 84: 747-778.
[2] Mac Latchy J. Metal data from base metal smelters and refineries. Environment Canada. 1992.
[3] Document de consultation publique 23 septembre Le chrome dans l'eau potable. 2015 **;** 90.
[4] Mamane O S, Zanguina A, Daou I, Natatou I**.** J. Soc. Ouest-Afr. Chim. 2016 **;** 041: 59 – 67.
[5] Al Bahri M, Calvo L, Gilarranz MA, Rodriguez JJ. **(**Activated carbon from grape seeds upon chemical activation with phosphoric acid: Application to the adsorption of diuron from water. Chemical Engineering Journal. 2012; 203, 348-356.
[6] Basta AH, Fierro V, Saied H, Celzard A**.** Effect of deashing rice straws on their derived activated carbons produced by phosphoric acid activation. Biomass and bioenergy. 2011; 35: 1954-1959.
[7] Fierro V, Muniz G, Basta AH, El-Saied H, Celzard A. Rice straw as precursor of activated carbons: activation by orthophosphoric acid. J. Hazard Mater. 2010; 181: 27-34.
[8] Mohan D, Singh KP, Singh VK. Wastewater treatment using lowcost activated carbons derived from agricultural byproducts-a case study. J. Hazard Mater. 2008; 152: 1045–1053.
[9] Diao Y, Walawender WP, Fan LT. Activated carbons prepared from phosphoric acid activation of grain sorghum. Bioresour. Technol. 2002; 81: 45–52.
[10] El Nemr A, Khaled A, Abdelwahab O, ElSikaily A. Treatment of wastewater containing toxic chromium using new activated carbon developed from date palm seed. J. Hazard. Mater. 2008; 152: 263–275.
[11] Demirbas E, Kobya M, Konukman, AES. Error analysis of equilibrium studies for the almond shell activated carbon adsorption of Cr (VI) from aqueous solutions. J. Hazard. Mater. 2008; 154:787–794.
[12] Cabal B, Budinova T, Ania CO, Tsyntsarski B, Parra JB, Petrova B. Adsorption of naphthalene from aqueous solution on activated carbons obtained from bean pods. J. Hazard. Mater. 2009; 161: 1150–1156.
[13] Díaz-Díez MA, Gómez-Serrano V, González CF, Cuerda-Correa EMA, Macías-García A. Appl. Surf. Sci. 2004; 238 (1–4): 309–313.
[14] Suárez-García F, Martínez-Alonso A, Tascón JMD. Microporous and Mesoporous Materials. 2004; 75 (1–2): 73–80.
[15] Rodriguez-Reinoso F, Molina-Sabio M. Activated carbons from lignocellulosic materials by chemical and/or physical activation: an overview Carbon. 1992; 30: 1111-1118.
[16] Carvalho AP, Gomes M, Mestre AS, Pires J, de Carvalho MB. Carbon. 2004; 42 (3): 672–674.
[17] Lei Yu, Yong-ming, luo. The adsorption mechanism of anionic and cationic dyes by Jerusalem artichoke stalk-based mesoporous activated carbon. J. Environ. Chem. Eng, 2014; 2: 220-229.
[18] Perrin A, Celzard A, Albiniak A, Kaczmarczyk J, Marêché JF, Furdin G. Carbon. 2004; 42 (14): 2855–2866.
[19] Derbyshire F, Jagtoyen M, Andrews R, Rao A, Martin-Gullon I, Grulke, EA, In Radovic LR. Ed. Chemistry and Physics of Carbon 27, New York: Marcel Dekker. 2001; 1–66.

[20] Mbaye G**.** Développement de charbon actif à partir de biomasse lignocellulosique pour des applications dans le traitement de l'eau". Thèse de doctorat en technologie de l'Eau, de l'Energie et de l'Environnement. 2iE, Burkina Faso. 2015 ; 215.
[21] Boehm H. Chemical Identification of Surface Groups. Academic Press. 1966; 179-274.
[22] Lopez-Ramon MV, Stoecklein F, Moreno-Castilla C, Carrasco-Marin F. On the Characterization of acidic and basic surface sites on carbons by various techniques", Carbon. 1999; 37: 1215-1221.
[23] Bestani B, Benderdouche N, Benstaali B, Belhakem M, Addou A. Bioresour. Technol. 2008; 99: 8441–8444.
[24] Adamson AW. Physical chemistry of surfaces 4 ème Edition. John wiley and sons: New York. 1982.
[25] Allen SJ, Mckay G, Khander KYH. Equilibrium adsorption isotherms for basic dyes onto lignite. J. Chemical Technology and Biotechnol. 1989; 45: 291.
[26] Kannan, and al. Kinetics and mechanism of removal of methylene blue by adsorption on various carbons-A comparative study. Dyes Pigments. 2001; 51: 25-40.
[27] Crank G. The mathematics of diffusion". Clarendon Press, London, New York. 1933.
[28] Langmuir I. The adsorption of gases on plane surfaces of glass, mica and platinium. Journal of Am. Chem. Soc. 1918; 40.
[29] Avom J, Mbadcam JK, Matip MRL, Germain P. Adsorption isotherme de l'acide acétique par des charbons d'origine végétale"; African Journal of Science and Technology (AJST); Science and Engineering Series. 2001; 2 (2): 1-7.
[30] Altinisik A, Gur E, Seki Y. A Natural Sorbent, Luffa Cylindrica for the Removal of a Model Basique Day; Journal of Hazardous Materials. 2010**;** 179: 658-664.
[31] De Wild PJ, Den Uil H, Reith JH, Kiel JHA, Heeres HJ**.** "Biomass valorisation by staged degasification". *J. Anal. Appl. Pyrolysis*, 2009; 85: 124–133.
[32] Haque MdM, Hasan M, Islam MdS, Ali MdE. Physico-mechanical properties of chemically treated palm and coir fibre reinforced polypropylene composites. *Bioresour.Technol*. 2009; 100: 4903–4906.
[33] Sinha S, Rout SK. Influence of fibre-surface treatment on structural, thermal and mechanical properties of jute. J. Mater. Sci. 2008; 43: 2590–2601.
[34] Maâzou SDB, Hima IH, Maman Mousbahou MA, Adamou Z, Ibrahim N. "Elimination du chrome par du charbon actif élaboré et caractérisé à partir de la coque du noyau de Balanites agyptiaca". Int. J. Biol. Chem. Sci. 2017; 11 (6): 3050-3065.
[35] Barrett EP, Joyner LJ, Halenda PH. The determination of pore volume and area distribution on porous solids I: computation from nitrogen isotherms. J, Amer, Chem, Soc. 1951; 73: 373-380.
[36] Mbaye G. Synthese et étude des charbons actifs pour le traitement des eaux usées d'une tannerie. Mémoire de master à l'Institut International d'Ingénierie de l'Eau et de l'environnement. 2009 ; 61.
[37] Aravindhan R, JRR, Nair BU. Preparation and characterization of activated carbon from marine macro-algal biomass. Journal of Hazardous Materials. 2009 ; 162: 688–694.
[38] Ousmaila SM, Adamou Z, Ibrahim D, Ibrahim N. Préparation et caractérisation de charbons actifs à base de coques de noyaux de Balanites Eagyptiaca et de Zizyphus Mauritiana. J. Soc. Ouest-Afr. Chim, 21ème. 2016; 041: 59 – 67**.**
[39] Tchieta PG, Mbouombouo JB, Magapgie NLC, Kede MC, Poumve Z H. Adsorption of Eriochrome Black T (EBT) Onto Activated Carbons Obtained from Cola Anomala Nut Shells by Chemical Activation with Phosphoric Acid (H3PO4). International Journal of Science and Research. 2019 ; 8: 2319-7064.
[40] Hamzeh Y, Ashori A, Azadeh E, Abdulkhani A. Removal of acid Orange 7 and remazol black 5 reactive dyes from aqueous solutions using a novel biosorbent. Mater. Sci. Eng. 2012; 32: 1394–1400.
[41] Khoulalene L, Semmar S. Étude Cinétique et Thermodynamique de l'Adsorption du Noir Erichrome T sur le Charbon. Memoire de Master Université A. Mira-Béjaia. 2016 ; 89.
[42] Bayrak Y, Yesiloglu Y, Gecgel U. Adsorption behavior of Cr (VI) on activated hazelnut shell ash and activated bentonite. Micropor. Mesopor. Mater. 2006 ; 91: 107-110.

[43] Serpen A, Atac B, Gökmen V. Adsorption of Maillard reaction products from aqueous solutions and sugar syrups using adsorbent resin. J. Food, Eng. 2007; 82:342 350.
[44] Ahmaruzzaman M, Sharma DK. Adsorption of phénols from wast water. J. Colloid Int, Sci. 2005; 287: 14-24.
[45] Bishnoi NR, and al. Adsorption of Cr (VI) on activated rice husk carbon and activated alumina. Bioresource Technology. 2004; 91(3): 305-307.
[46] YS, H. Review of second-order models for adsorption systems. Journal of Hazardous Materials, B 2006; 136: 681-689.
[47] Lei Yu, Yong-ming luo. The adsorption mechanism of anionic and cationic dyes by Jerusalem artichoke stalk-based mesoporous activated carbon. J. Environ. Chem. Eng. 2014; 2: 220-229.
[48] Errais E. Réactivité de surface d'argile naturelle: Etude de l'adsorption de colorants anioniques. Thèse de doctorat. Université de strasbourg. 2011.